Energy Gaps in Supramolecular Functionalized Graphene Nanoribbons

Alexis Nduwimana and Xiao-Qian Wang*

Department of Physics and Center for Functional Nanoscale Materials, Clark Atlanta University, Atlanta, Georgia 30314

ARTICLE

ABSTRACT The electronic structure characteristics of supramolecular functionalization of graphene nanoribbons with π-conjugated polymers are investigated using first-principles density functional theory. Noncovalent polymer functionalization leads to distinct changes in the electronic properties, particularly the band gaps of metallic and semimetallic graphene nanoribbons. A detailed analysis of band alignments reveals a profound level hybridization for ribbons with various shaped edges and spin density waves near the edges of zigzag ribbons. The extracted planar polymer conformations and the disappearance of the metallic behavior are in conformity with experimental observations.

KEYWORDS: graphene · nanoribbon · band gap · first-principles calculations · functionalization

Graphene, a single sheet of graphite, is an emerging new material for nanoelectronic devices and holds the potential to be the successor to silicon.[1−5] As a truly two-dimensional system and a zero-gap semiconductor, where the carriers behave as massless fermions, graphene possesses a number of remarkable electronic properties such as tunable carrier type and density,[4] exceptionally high carrier mobility,[5] and quantization of the conductivity,[1] making it ideal for use in nanoelectronics. On the other hand, silicon has fundamental limitations inhibiting operation in ever-shrinking device sizes used in microelectronics, optics, and sensors.[5]

Bringing graphene to the level of a technologically relevant material depends upon improved understanding and control of the structure and properties of this novel material.[1−5] The properties of graphene-based nanostructures can be modified and controlled by the introduction of functionalized chemical groups.[12] In order to utilize their remarkable electrical characteristics, it would be highly desirable to understand the associated electronic structures. In this regard, intensive efforts are being made to explore the properties of functionalized graphene nanostructures.

By patterning graphene into a narrow ribbon structure, the carriers are laterally confined to form a quasi-one-dimensional (1D) system, similar to the case of single-walled carbon nanotubes (SWNTs).[7−9] Graphene nanoribbons (GNRs) can be considered as unrolled SWNTs and are advantageous over nanotubes for electronics owing to the planar 2D structure that enables circuit design with standard lithography techniques.[7−9] Graphene can be cut with different shapes and selected edge direction. The formation of associated 1D subbands is expected to yield an energy gap for certain ribbon widths and crystallographic directions.[10,11] By tailoring the ribbon width, it is possible to design semiconductor GNRs with a tunable band gap.[5,6] The fundamental issue of band gap engineering in GNRs has been recently addressed in several experimental studies.[6,12] The conductance of the GNR depends crucially on the edge structures,[12] and noncovalent polymer-functionalized GNRs exhibit all-semiconducting behavior,[6] in contrast to SWNTs that contain about one-third metallic species. It is clear that the confinement in edges and noncovalent polymer functionalization are responsible for these observations, but the origin of this remarkable all-semiconducting behavior is not fully understood.

The modular structure and hierarchical assembly properties of π-conjugated polymers make these macromolecules very attractive to the rational design of nanomaterials *via* supramolecular functionalization.[13] The chromophore backbone or side chain of the polymers can form a uniquely

*Address correspondence to xwang@cau.edu.

Received for review April 28, 2009 and accepted June 17, 2009.

Published online June 23, 2009.
10.1021/nn9004268 CCC: $40.75

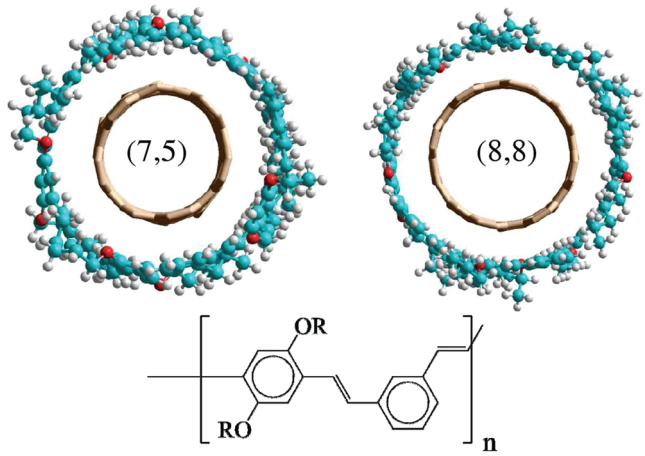

Figure 1. Chemical structure of a PmPV unit, where R is the side chain used in experiments such as C_8H_{17} or C_6H_{13}, along with the top view of the PmPV wrapping around semiconducting (7,5) and metallic (8,8) nanotubes. Carbon, hydrogen, and oxygen atoms on the PmPV are represented with blue, white, and red, respectively.

ordered three-dimensional structure and be tailored to exhibit the suitable affinity to achieve improved dispersion. Poly[(*m*-phenylene vinylene)-*alt*-(*p*-phenylene vinylene)] (PmPV) (see Figure 1), the most studied polymeric dispersing reagent and capable of forming a helical conformation to embrace SWNTs of certain diameters,[13] effectively disperse sub-10 nm GNRs with ultrasmooth edges.[6] The solution-phase-derived GNRs stably suspend in solvents with noncovalent PmPV functionalization, which afford outstanding graphene field effect transistors.[6]

Quantitative understanding of charge transfer at the interface and the spatial distribution of the resulting charge carriers is a critical input to device design. Here we present a comprehensive investigation of structural and electronic properties of PmPV-functionalized GNRs. Our results show that the $\pi-\pi$ interaction between the PmPV and the GNRs manifests itself *via* the formation of planar PmPV conformations. First-principles calculations on the electronic structures further reveal that there exists profound level hybridization for the PmPV-functionalized GNRs, which leads to distinct changes in the electronic properties, particularly the band gap opening for metallic and semimetallic GNRs.

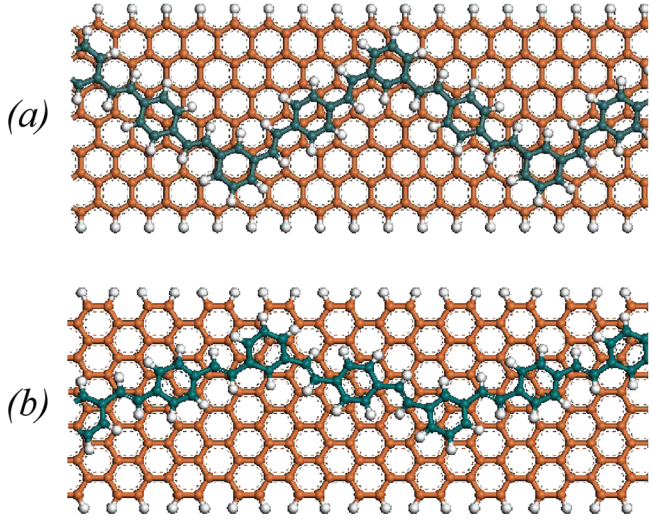

Figure 2. Top view of optimized structure of PmPV-functionalized 7-ZGNR (a) and 12-AGNR (b). The carbon atoms at the PmPV and GNR are colored with dark green and amber, respectively. The side chains of the PmPV are replaced with hydrogen in first-principle calculations for simplicity, as the effect of side chain on electronic structure is not important.[6,13]

We have employed a combination of force-field-based molecular dynamics (MD)[14] and first-principles density functional calculations with plane wave basis[15] to investigate the structural and electronic properties of PmPV-functionalized GNRs. Force-field-based MD[14] was used to prescreen molecular geometries, and first-principles calculations[15] were employed to determine the electronic structure of functionalized GNRs. Periodic boundary conditions were employed in the *x* direction with a supercell large enough to eliminate the interaction between neighboring GNRs. An energy cutoff of 300 eV was sufficient to converge the grid integration of the charge density, and the Monkhorst–Pack *k*-point mesh of $7 \times 1 \times 1$ was found to provide sufficient accuracy in the Brillouin zone integration. The structures were obtained by fully minimizing the forces and stress in first-principles calculations with forces less than 0.01 eV/Å. Although the local density approximation[16] to the density functional theory underestimates the band gap, the many-body correction is smaller for sp^2 than for sp^3 configurations.[17]

One of the fundamental issues is how the noncovalent interaction affects the PmPV conformations. As a test case, we have employed the simulation approach to the study of noncovalent functionalization of PmPV helically wrapping around the SWNTs. The helical conformation of the π-conjugated backbone of PmPV forms a defined cavity (~1.5 nm in diameter), which provides a favorable environment to selectively host SWNTs of comparable diameters.[13] Our MD calculation results demonstrate that the semirigid π-conjugated polymer backbone has certain flexibility to adjust its conformation during wrapping, and the wrapped polymer successfully adopts a helical conformation.[13] As shown in Figure 1, the phenylene vinylene (PV) fragments are arranged either perpendicular or parallel to the SWNT surface in the assembly process to facilitate $\pi-\pi$ interactions. The optimized structure favors parallel configurations. Furthermore, the functionalized SWNTs preserve the integrity of the electronic structure of pristine semiconducting and metallic SWNTs in that there exists a paucity of modification in the charge distribution of states near the Fermi level.

The GNRs involved in the present study were constructed based on sp^2 hybridization model. In order to study intrinsic properties, the edges of the ribbons were passivated by hydrogen atoms, resulting in neutral bond saturated GNRs. The initial value of 1.42 and 1.10

TABLE 1. Calculated Ribbon Width (W_R), PmPV Width (W_P), Angle of the PmPV Ridges (θ), Unit Cell Length (d), Average Distance between the Ribbon and the PmPV (d_{R-P}), Band Gap of Pristine GNRs (E_g^0), Gap of PmPV-Functionalized GNRs (E_g)

	10-AGNR	11-AGNR	12-AGNR	7-ZGNR	8-ZGNR
W_R (Å)	11.0	12.2	13.5	13.5	15.5
W_P (Å)	4.2	4.1	4.1	7.3	7.3
θ (°)	144	145	145	113	113
d (Å)	22.6	22.6	22.6	22.1	22.1
d_{R-P} (Å)	3.44	3.43	3.43	3.38	3.41
E_g^0 (eV)	1.12	0.12	0.57	0.33	0.33
E_g (eV)	1.15	0.24	0.59	0.28	0.27

Å was used for C−C and C−H bonds, respectively. The armchair and zigzag structures of GNRs as seen in Figure 2 were constructed by cutting an infinite graphene sheet along the (n,n) and (n,0) directions, respectively. The naming of the armchair and zigzag GNRs (AGNR and ZGNR) follows the edge structure nomenclature,[10,11] such that an armchair (zigzag) tube unfolds into a zigzag (armchair) ribbon. Intensive MD simulation study indicates that the PmPV polymer possesses flat planar geometries that are spontaneously attracted to the GNRs, in agreement with experimental observation of a uniform PmPV suspension.[6] The ridge shaped PmPV suspension facilitates planar π−π interactions, which is the counterpart of the helical wrapping pattern on SWNTs. The structures obtained from force-field-based MD calculations are further fully optimized using the first-principles method. The structural parameters of the optimized GNRs are summarized in Table 1. The average distance between the GNRs and the PmPV is around 3.4 Å, about twice the van der Waals radius of carbon. The noncovalent polymer functionalization induces slight distortion to the flat ribbon due to the existence of edges. However, the PmPV can successfully adjust the torsion angles to facilitate the planar π−π interactions. The effect of distortion on the extracted binding energy diminishes with increase of the ribbon width. Careful examination of the binding between the PmPV and GNRs of various shaped edges suggests that there is no preferred alignments for the PmPV polymer interacting GNRs with various shaped edges.

The energy gaps that open at the Fermi level depend on the ribbon width and the details of the ribbon edge geometry and termination. Our results of the band structures of pristine GNRs are consistent with previous theoretical studies.[10,11] Previous theoretical studies have shown that the band gap of ultrathin GNR with armchair edges generally opens up due to the quantum confinement and the edge bond relaxation. The oscillatory band gap for GNR with armchair edges (or the fact that the E_g^0 value for 11-AGNR is between the values for 10-AGNR and 12-AGNR) can be explained by the Fermi wavelength in the direction normal to the ribbon direction. Similar to zigzag SWNTs, the band gaps of AGNRs are divided into three groups, with the $3p + 2$, $3p + 1$, and $3p$ group (p is a positive integer) having a small, medium, and large gap, respectively. For each group, the gaps decrease with increasing width, w, in an approximate $1/w$ fashion.[10,11]

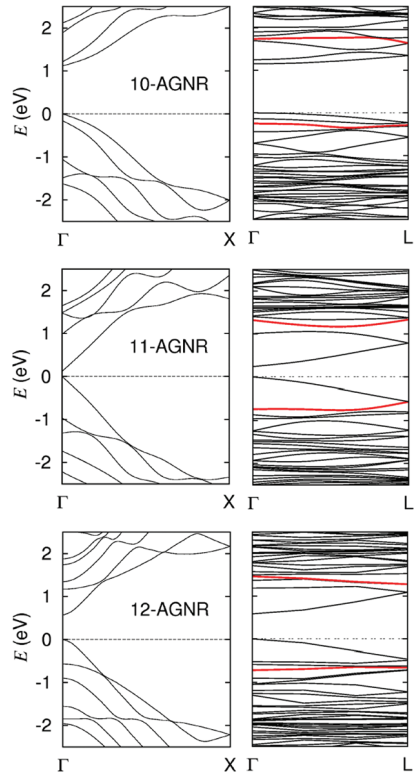

Figure 3. Calculated band structures of pristine (left panel) and functionalized (right panel) AGNRs. The PmPV-derived bands are colored red; $X = \pi/a$ and $L = \pi/d$, where $a = 2.46$ Å and $d = 22.6$ Å.

The characteristic features of band structures of the PmPV-functionalized AGNRs are shown in Figure 3 along with those of pristine AGNRs for comparison. The three AGNRs presented, 10-AGNR, 11-AGNR, and 12-AGNR, are representative cases for $3p + 1$, $3p + 2$,

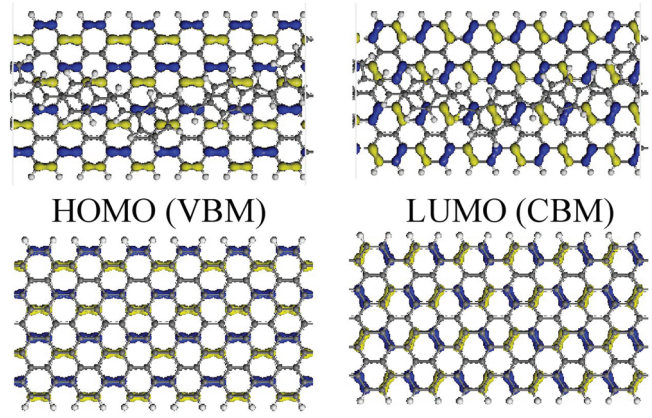

Figure 4. Charge density (blue) for VBM and CBM of PmPV-functionalized 11-AGNR (top panel) as compared to that of the pristine one (bottom panel). The sign of the wave function is indicated by light blue and yellow regions, respectively. The isovalue is 0.02 au.

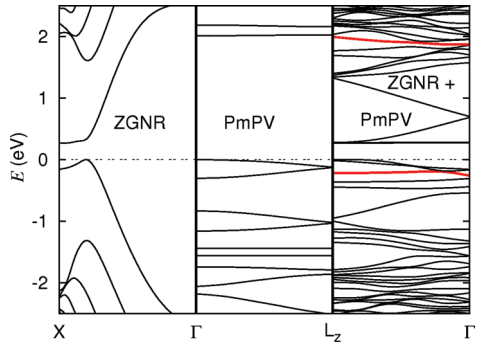

Figure 5. Calculated band structures of the spin-polarized 8-ZGNR (left panel), a periodic structured PmPV (central panel), and the spin-polarized PmPV-functionalized 8-ZGNR (right panel). PmPV-derived bands are colored red; $X = \pi/a$ and $L_z = \pi/d$, where $a = 2.46$ Å and $d = 22.1$ Å. The VBM (dash-dotted line) is set to zero.

and 3*p* AGNRs, respectively. In connection with the distinct edge bond relaxations, the oscillatory band gap feature for the three cases can be readily observable in Table 1. The functionalized AGNRs have larger unit cells. As a result, the bands fold the pristine ones in accordance with the smaller reciprocal space mesh. While there is a paucity of modifications for the gap of 3*p* and 3*p* + 1 PmPV-functionalized AGNRs, the band gap doubles for the 11-AGNR with the PmPV functionalization. In all the cases, the band gap remains direct at Γ for pristine and PmPV-functionalized AGNRs.

The band alignment between the GNR and the PmPV is based on the lineup of charge neutrality levels of the two components.[18,19] The gap between the highest-occupied molecular orbital (HOMO) and the lowest-unoccupied molecular orbital (LUMO) for the PmPV is 2.1 eV. The corresponding PmPV-derived states are shown as red lines in Figure 3. In all such cases, the band alignment is type-I such that charge carriers in valence band maximum (VBM) and conduction band minimum (CBM) accumulate in the AGNRs. In the absence of edge bond relaxation, the 3*p* + 2 group would exhibit a zero gap to be metallic, analogous to their SWNT counterpart.[10,17] However, because the effective ribbon width (the distance between the two nodal points at the edge) is not exactly in conformity with the corresponding wave vector associated with the Fermi point of graphene, a small gap opens up. This correlates to different overlaps at the edge. In order to substantiate this, we depict the charge density of the VBM and the CBM in Figure 4 for pristine and PmPV-functionalized AGNRs. As the functionalization leads to similar charge density distributions for the VBM and CBM states, the increase of the band gap due to noncovalent PmPV functionalization is mainly attributed to the enhanced mismatch in the Fermi wavelength, which arises from the unique 3D structure of the polymer−GNR nanohybrid. Closer scrutiny of the energetics contribution indicates that the edges quench the kinetic energy of the itinerant carriers and leads to the flat bands.

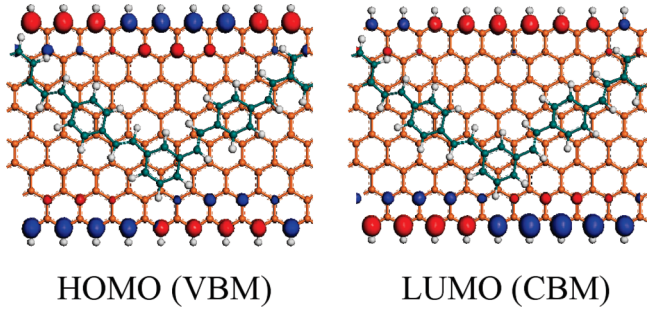

Figure 6. Charge density (blue for spin up and red for spin down) for the VBM and CBM states of the PmPV-functionalized 8-ZGNR.

An important ramification of present simulation results for AGNRs is the verification of all-semiconducting behavior for armchair and chiral GNRs, along with the lessened oscillatory band gap feature. The SWNT counterparts refer to zigzag and chiral tubes, which are either semiconducting or semimetallic depending upon the chiral indices (*n*,*m*). While the band alignment analysis indicates a similar type-I line up for SWNTs and GNRs,[18] the edge bond relaxation and noncovalent PmPV functionalization prompt an increase of the band gap for semimetallic GNR species. As a consequence, in order to confirm all-semiconducting behavior of functionalized GNRs observed experimentally, we are left to examine electronic characteristics of functionalized ZGNRs.

Armchair SWNTs are truly metallic due to the indirect overlap of π and π* bands.[21] The metallic armchair tubes may open up a pseudogap due to breaking of rotational symmetry in bundled samples.[21] Constructed through unfolding armchair SWNTs, ZGNRs have metallic ground state within spin-restricted calculations, and the minor distortion to the ZGNR due to PmPV functionalization does not lead to the opening of an energy gap. However, spin-polarized calculations reveal an energy gap due to the staggered magnetization of bipartition A and B lattices, consistent with previous calculations.[10,11,20] Zigzag edges contain either all A or all B sites, and a half-metallicity state[22] can be realized when an external electric field is applied across the ribbon. Of particular interest is whether the magnetic states can be sustained with noncovalent polymer functionalization since the functionalization breaks the symmetry of the A and B sublattices. We illustrate in Figure 5 the band structures of the pristine and PmPV-functionalized 8-ZGNR, together with the band structure of π-conjugated PmPV for the band alignment analysis. Both pristine and functionalized ZGNRs have spin-degenerate dispersions. The functionalized ZGNRs have a direct gap at the band edge. The resulting conduction band is flat due to the band folding of the flat band of the pristine ZGNR. The flat band feature can also be seen for the VBM state, which is indicative of localized states. As shown in Figure 6, the spin-polarized charge density of PmPV-functionalized 8-ZGNRs is con-

fined at edge of the ZGNR for VBM and CBM. It is worth noting that the symmetry of charge distributions between the A and B sublattice edges is broken, depending on the location of the PmPV. In contrast to the staggered magnetism in bipartition lattices, the spin up and spin down alternates on each side of the ZGNRs. The spin alternative creates what is known as spin density waves and has a characteristic wavelength of 1.96 nm. The spin density wave state is 0.013 eV lower in energy per edge atom than the paramagnetic state.

In conclusion, we have presented comprehensive studies for the electronic structure of PmPV-functionalized GNRs. The important role of the edge bond relaxation and the noncovalent functionalization on electronic structure characteristics is investigated. For ZGNR, the ground state changes from 2D staggered antiferromagnetic state for pristine ribbons to the edge-confined spin density wave state for the PmPV-functionalized ZGNRs. Our results demonstrate that noncovalent polymer functionalization could be used to tailor the band gap of a fixed GNR width, resulting in the enhancement of device performances. We remark, before closing, that it is straightforward to employ this approach to novel noncovalent functionalizations with a variety of π-conjugated polymers, and the investigation of the relevant electronic structures will provide an invaluable tool for developing graphene-based nanodevices.

Acknowledgment. This work was supported in part by the National Science Foundation (Grant No. DMR-02-05328) and Army Research Office (Grant No. W911NF-06-1-0442).

REFERENCES AND NOTES

1. Novoselov, K. S.; Geim, A. K.; Morozov, S. V.; Jiang, D.; Zhang, Y.; Dubonos, S. V.; Grigorieva, I. V.; Firsov, A. A. Electric Field Effect in Atomically Thin Carbon Films. *Science* **2004**, *306*, 666.
2. Zhang, Y.; Jiang, Z.; Small, J. P.; Purewal, M. S.; Tan, Y.-W.; Fazlollahi, M.; Chudow, J. D.; Jaszczak, J. A.; Stormer, H. L.; Kim, P. Landau-Level Splitting in Graphene in High Magnetic Fields. *Phys. Rev. Lett.* **2006**, *96*, 136806.
3. Novoselov, K. S.; Geim, A. K.; Morozov, S. V.; Jiang, D.; Katsnelson, M. I.; Grigorieva, I. V.; Dubonos, S. V.; Firsov, A. A. Two-Dimensional Gas of Massless Dirac Fermions in Graphene. *Nature* **2005**, *438*, 197.
4. Pereira, V. M.; Guinea, F.; Lopes dos Santos, M. B.; Peres, N. M. R.; Castro Neto, A. H. Disorder Induced Localized States in Graphene. *Phys. Rev. Lett.* **2006**, *96*, 036801.
5. Berger, C.; Song, Z.; Li, X.; Wu, X.; Brown, N.; Naud, C.; Mayou, D.; Li, T.; Hass, J.; Marchenkov, A. N.; Conrad, E. H; First, P. N.; de Heer, W. A. Electronic Confinement and Coherence in Patterned Epitaxial Graphene. *Science* **2006**, *312*, 1191.
6. Li, X.; Wang, X.; Zhang, L.; Lee, S.; Dai, H. Chemically Derived, Ultrasmooth Graphene Nanoribbon Semiconductors. *Science* **2008**, *319*, 1229.
7. Geim, A. K.; Morozov, S. V.; Hill, E. W.; Blake, P.; Katsnelson, M. I.; Novoselov, K. S. Detection of Individual Gas Molecules Adsorbed on Graphene. *Nat. Mater.* **2007**, *6*, 652.
8. Wehling, T. O.; Novoselov, K. S.; Morozov, S. V.; Vdovin, E. E.; Katsnelson, M. I.; Geim, A. K.; Lichtenstein, A. I. Molecular Doping of Graphene. *Nano Lett.* **2008**, *8*, 173.
9. Elias, D. C.; Nair, R. R.; Mohiuddin, T. M. G.; Morozov, S. V.; Blake, P.; Halsall, M. P.; Ferrari, A. C.; Boukhvalov, D. W.; Katsnelson, M. I.; Geim, A. K.; Novoselov, K. S. Control of Graphene's Properties by Reversible Hydrogenation: Evidence for Graphane. *Science* **2009**, *323*, 610.
10. Son, Y.-W.; Cohen, M. L.; Louie, S. G. Energy Gaps in Graphene Nanoribbons. *Phys. Rev. Lett.* **2006**, *97*, 216803.
11. Barone, V.; Hod, O.; Scuseria, G. E. Electronic Structure and Stability of Semiconducting Graphene Nanoribbons. *Nano. Lett.* **2006**, *6*, 2748.
12. Zhou, S. Y.; Gweon, G. H.; Fedorov, A. V.; First, P. N.; de Heer, W. A.; Lee, D. H.; Guiner, F.; Neto, A. H. C.; Lanzara, A. A. Substrate-Induced Bandgap Opening in Epitaxial Graphene. *Nat. Mater.* **2007**, *6*, 916.
13. Yi, W.; Malkovskiy, A.; Chu, Q.; Sokolov, A. P.; Colon, M. L.; Meador, M.; Pang, Y. Wrapping of Single-Walled Carbon Nanotubes by a π-Conjugated Polymer: The Role of Polymer Conformation-Controlled Size Selectivity. *J. Phys. Chem. B* **2008**, *112*, 12263.
14. Jensen, F. *Introduction to Computational Chemistry*, 2nd ed; John Wiley & Sons: Hoboken, NJ, 2006; pp 1−624.
15. Kresse, G.; Furthmuller, J. Efficient Iterative Schemes for *Ab Initio* Total-Energy Calculations Using a Plane-Wave Basis Set. *Phys. Rev. B* **1996**, *54*, 11169.
16. Becke, A. D. Density-Functional Exchange-Energy Approximation with Correct Asymptotic Behavior. *Phys. Rev. A* **1988**, *38*, 3098.
17. Yang, L.; Cohen, L. M.; Louie, G. S. Magnetic Edge-State Excitons in Zigzag Graphene Nanoribbons. *Phys. Rev. Lett.* **2008**, *101*, 186401.
18. Ogunro, O.; Wang, X.-Q. Quantum Electronic Stability in Selective Enrichment of Carbon Nanotubes. *Nano Lett.* **2009**, *9*, 1034.
19. Nduwimana, A.; Musin, R. N.; Smith, A. M.; Wang, X.-Q. Spatial Carrier Confinement in Core−Shell and Multishell Nanowire Heterostructures. *Nano Lett.* **2008**, *8*, 3341.
20. Wimmer, M.; Adagideli, I.; Berber, S.; Tomanek, D.; Richter, K. Spin Currents in Rough Graphene Nanoribbons: Universal Fluctuations and Spin Injection. *Phys. Rev. Lett.* **2008**, *100*, 177207.
21. Ouyang, M.; Huang, J.-L.; Cheung, C. L.; Lieber, C. M. Energy Gaps in "Metallic" Single-Walled Carbon Nanotubes. *Science* **2001**, *292*, 702.
22. Son, Y.-W; Cohen, L. M.; Louie, G. S. Half-Metallic Graphene Nanoribbons. *Nature* **2006**, *444*, 347.